

Nature of ordering in Potts spin glasses

Jayanth R. Banavar

Department of Physics and Materials Research Laboratory, Pennsylvania State University, University Park, Pennsylvania 16802

Marek Cieplak*

Department of Physics and Astronomy, The Johns Hopkins University, Baltimore, Maryland 21218

(Received 30 January 1989)

The zero-temperature scaling approach is applied to the three-state Potts spin glass. Our results suggest that the $\pm J$ model has a lower critical dimensionality greater than 3, whereas for the Gaussian model this dimensionality is slightly less than 3. The $T=0$ scaling exponents are estimated in $D=2$ and 3. The results are based mostly on exact transfer-matrix calculations and on a Monte Carlo quenching procedure.

I. INTRODUCTION

Potts models^{1,2} have proved to be of great interest in studies of phase transitions. The Hamiltonian for the p -state Potts model is given by

$$H = - \sum_{\langle ij \rangle}^N J_{ij} \delta_{S_i, S_j}, \quad (1)$$

where $\langle ij \rangle$ denotes a summation over nearest neighbors, $\delta_{\alpha, \beta}$ is the Kronecker delta, and the spin S_i takes on one of the values $1, 2, 3, \dots, p$. The spins are located on the sites of a D -dimensional lattice. J_{ij} is greater than zero for the ferromagnetic case and less than zero for the antiferromagnetic one. For $p=2$, Eq. (1) reduces to the Ising model (with a redefined J).

The properties of the ferromagnetic model are now well understood.² The system is paramagnetic at high temperatures and undergoes a phase transition to a ferromagnetically ordered state at low T for all $p \geq 2$ with the lower critical dimensionality (LCD) being equal to 1. In the antiferromagnetic case the residual entropy in the ground state may lead to complex ordering. It is known³ that for $p=3$ the LCD is equal to 2. The low- T phase for a simple-cubic (sc) lattice shows a sublattice ordering for $p \leq 4$.⁴

Recently, there has been considerable interest in studies of Potts models with quenched disorder. In particular, Potts spin glasses (PSG) are considered to have features which may help in understanding the liquid-glass transition.⁵ PSG may also describe anisotropic orientational glasses⁶ in which the quadrupole moment is pinned to one of p discrete directions.

The PSG with infinite-range interactions has been thoroughly analyzed and leads to rich behavior.⁷ In particular, it is known that this model, depending on the temperature, has two different types of spin-glass ordering for any value of p . The two distinct PSG phases differ in the nature of overlaps between the ground states of the system. In actual physical applications, however, models with short-range interactions are more likely to be of relevance.

Monte Carlo studies of the short-ranged PSG's have been carried out by Carmesin and Binder.⁸ They have considered the case of Gaussian couplings (zero mean, unit dispersion). They find that in $D=3$ the system is very close to its LCD. This means that the critical temperature, T_c , for the paramagnet spin-glass transition, if nonzero, is probably rather small. The dynamics of this system is slow and it is of the Kohlrausch type.

An analysis of the PSG using the Migdal-Kadanoff renormalization group suggests no conventional spin-glass behavior.⁹ This conclusion, however, may be an artifact of the hierarchical lattice considered for which the scaling scheme is exact.

Recently, much progress has been made in the studies of Ising spin glasses (ISG) using a technique called $T=0$ scaling.¹⁰⁻¹⁴ The $T=0$ scaling approach is a simple yet powerful method of studying systems with no obvious long-range order. It is based on the phenomenological observation that for all $T < T_c$ the behavior of a system at long length scales should be governed by a $T=0$ fixed point. This approach has proved to be particularly effective in the case of short-range Ising and Heisenberg spin glasses. Its basic prediction has been that the $D=3$ Heisenberg spin glass does not undergo an equilibrium spin-glass-paramagnet transition, at a nonzero T_c , whereas the $D=3$ ISG does have a transition. These results have been subsequently confirmed by detailed Monte Carlo simulations.¹⁵⁻¹⁷ An Imry-Ma-type¹⁸ analysis based on plausible assumptions^{12,19,20} has led to several novel predictions in the low- T phase, many of which are at odds with a mean-field analysis of the infinite-range model.¹⁵

The basic concept of the $T=0$ scaling theory is that of a scaling stiffness or a scale-dependent coupling energy, $\delta E(L)$. This coupling is determined by studying the sensitivity to boundary conditions¹⁰⁻¹³ of the ground-state energy of finite blocks of length L . $\delta E(L)$ is a characteristic measure of that sensitivity. In the ordered phase at $T=0$

$$\delta E(L) \approx L^y. \quad (2)$$

For systems below the LCD, y is negative and a phase transition occurs at $T=0$. On the other hand, above the LCD, y is positive and the transition occurs at a nonzero T_c . Below T_c Eq. (2) holds for the free-energy sensitivity to boundary conditions:

$$\delta F(L) \approx Y(T)L^y, \quad (3)$$

where $Y(T)$ vanishes at T_c as a power law²¹ and the exponent y is governed by the $T=0$ fixed point. In the paramagnetic phase $\delta F(L)$ should decay exponentially with the size of the system.

For systems above the LCD the exponent y determines the power-law decay of nonlinear correlations in the ordered phase^{12,19} and the nonanalytic dependence of the magnetization on the magnetic field.¹² For systems below the LCD the correlation length diverges as $T \rightarrow 0$. The exponent of this divergence is given by $\nu = -1/y$.

In this paper we present the results of a comprehensive study of the three-state PSG's using the $T=0$ scaling approach to in $D=2$ and 3. Our results suggest that the Gaussian PSG (GPSG) has an LCD slightly less than 3 and therefore in three dimensions (3D) it has a nonzero T_c . On the other hand, the bimodal PSG (BPSG) with the exchange constant J_{ij} given by the distribution

$$P(J_{ij}) = \frac{1}{2}[\delta(J_{ij}-1) + \delta(J_{ij}+1)]$$

has an LCD which is probably greater than 3. We have also determined the $T=0$ scaling exponents for the 2D BPSG and GPSG which are both below the LCD. A brief account of our results has recently appeared in the literature.²² It should be noted that the $T=0$ scaling approach predicts that the LCD of a ferromagnetic Potts model is 1 for $p > -2$.

In Sec. II we describe the notation used in the paper. Most of our calculations were done using a transfer-matrix method which we present in Sec. III. In Sec. IV we discuss the complementary method of finding ground states—that of Monte Carlo quenching. In Sec. V we present results on the exponent y in PSG's. In Sec. VI we study the probability distribution of ΔE and derive the exponent η (the latter for the 2D BPSG). In Sec. VII we discuss the calculation of an effective fractal dimensionality of the domain-wall interface. This dimensionality characterizes the scaling behavior of the interfacial entropy and determines the chaotic nature of the ordered state of the PSG. Finally, in Sec. VIII, we estimate the critical temperature for the 3D GPSG using the transfer-matrix method.

II. SENSITIVITY TO BOUNDARY CONDITIONS: DEFINITIONS

In order to study the sensitivity to boundary conditions we consider blocks of $A(l+1)$ Potts spins. The parameter A is the transverse area of the sample and l its length in the direction in which differing boundary conditions are applied. For cubic samples $l=L$ and $A=L^{D-1}$. In what follows the symbol L denotes the length of hypercubic samples. We reserve the symbols l and A for situations when one of these parameters is varying and the other is fixed.

In the planar ($D-1$) directions periodic boundary conditions are applied. In the longitudinal direction, the spins in the first and last column ($D=2$) or plane ($D=3$) are fixed randomly in one of the three states. This mimics the influence of neighboring blocks on the finite block under study. The domain wall is created by turning the spin states on one boundary (1 into 2, 2 into 3, 3 into 1) with the spins on the other boundary held fixed. The difference in the ground-state energies is denoted by ΔE . It can be either positive or negative; we define δE

$$\delta E = \langle |\Delta E| \rangle_c, \quad (4)$$

where $\langle \dots \rangle_c$ denotes the configurational average over samples.

Another way of defining δE would be to consider the root mean square ΔE . As in the case of ISG, however, we expect the same scaling behavior for both quantities.

III. THE TRANSFER-MATRIX METHOD

Our calculations were done using an extension to Potts spins of the transfer-matrix method used by Bray and Moore¹² ($T=0$) and Morgenstern and Binder²³ ($T>0$) for their studies of ISG. In order to illustrate this method we consider the $D=2$ three-state Potts model. With the boundary conditions taken into account, the Hamiltonian (1) can be rewritten as

$$H = - \sum_{x=1}^l \sum_{y=1}^A J_{x,y;x+1,y}^{(l)} \delta_{S_{x,y}, S_{x+1,y}} - \sum_{x=1}^l \sum_{y=1}^A J_{x,y;x,y+1}^{(A)} \delta_{S_{x,y}, S_{x,y+1}}, \quad (5)$$

where $S_{x,A+1} = S_{x,1}$. Spins $S_{1,y}$ and $S_{l+1,y}$ are fixed in randomly selected states. The superscripts (l) and (A) in the exchange couplings help one to distinguish between longitudinal and “planar” couplings. Our task here is to scan through all of the states of the system and to select the state of lowest energy.

The first step in the procedure is to set $x=1$ and to enumerate all 3^A states in the first column of “area” A . The corresponding energies are $e_1(\nu)$, where $\nu = 1, \dots, 3^A$. Now we treat the “interplane” couplings with $x=1$ and $x=2$. We focus first on spin $S_{1,1}$. It couples to $S_{2,1}$ in the second layer via $J_{1,1;2,1}^{(l)}$. For each of the three states of $S_{2,1}$ there are three possible states of $S_{1,1}$. In a $T=0$ calculation we select the lowest of the latter and modify the energy of each spin configuration of the first “plane” accordingly.

At this stage there are no degrees of freedom attached to $S_{1,1}$. The spin $S_{2,1}$ takes the place of $S_{1,1}$ whereas $S_{1,1}$ adjusts itself to give the lowest-energy configuration. In the same fashion the spin $S_{1,2}$ is eliminated in favor of $S_{2,2}$. This “zipping” action continues until there are no degrees of freedom in the first plane. At this stage there are again 3^A states with energies $e'_1(\nu)$.

The next step is to take care of the “planar” couplings in the second column. Again we enumerate all states on the second column and add the corresponding energy contributions to $e'_1(\nu)$ to obtain the effective energies

$e_2(\nu)$ for states in the second column. This includes automatic best adjustments of spins in the first column.

We proceed in this way until all spins are taken into account. Instead of dealing with 3^{4l} states the transfer-matrix approach enables one to keep track of only 3^4 of these. At the end the corresponding energies are $e_1(\nu)$. The lowest of these is the ground-state energy.

A finite- T transfer-matrix calculation of the free energy proceeds similar to the approach outlined by Morgenstern and Binder.²³ Briefly, instead of adding subsequent contributions to the energy, one multiplies the corresponding Boltzmann factors. Instead of selecting the lowest local state, when “zipping,” one adds Boltzmann weights corresponding to all of the states of the spin undergoing “extinction.” Finally, one calculates a logarithm of the partition function. There is one technical difficulty in this method: a string of large or small Boltzmann factors, when multiplied term by term, may give rise to numerically uncontrollable numbers. To avoid this problem we perform divisions or multiplications of the results by powers of ten, which are then reinserted after taking the final logarithm.

A transfer-matrix calculation for $D=3$ is similar to the 2D method outlined above. Instead of dealing with the column states, as the basic ingredients, one has to consider all the states in each plane of area A . In practice, this restricts us to A not exceeding 3×3 . In order to study $4 \times 4 \times 4$ systems we have to resort to approximate methods, such as Monte Carlo quenching.

IV. MONTE CARLO QUENCHING

McMillan¹³ in his “domain-wall renormalization-group” version of the $T=0$ scaling theory of ISG has suggested a simple scheme for determination of ground states. This scheme goes as follows: one first equilibrates the system at a temperature T_i and then runs the system over M Monte Carlo updates per spin with $M=2^m$, $m=1,2,\dots,m_0$. After each update the system is quenched to $T=0$ and the energy is noted. For each sample the procedure is repeated with the turned boundary conditions. For each m , the lowest energy visited is taken to approximate the true ground state and $\Delta E(m)$ is obtained. $\delta E(L,m) = \langle |\Delta E(m)| \rangle$ should then be extrapolated to $m \rightarrow \infty$ to obtain a measure of $\delta E(L)$. McMillan considered 40 000 samples of ISG in the 3D case. For $L=3$ and 4 he took $m_0=10$ and 11, respectively, and sought an exponential extrapolation to the convergence.

Our approach to quenches in PSG’s is to consider smaller number of samples but to select m_0 large enough so that the convergence at a constant value is actually established. Results for the GPSG are shown in Fig. 1. We took $T_i=0.4$ which yielded a success rate of 60% for the spin-flip attempts. For $L=4$ and 3 we considered 500 and 1000 samples, respectively. In both cases $m_0=14$. It is seen, however, that for $L=3$, $m_0=9$ is sufficient to obtain convergence. For $L=4$ the saturation is reached at $m=13$. The converged $L=3$ final data point agrees with the exactly obtained transfer-matrix result of 0.701 ± 0.004 based on 10 000 samples.

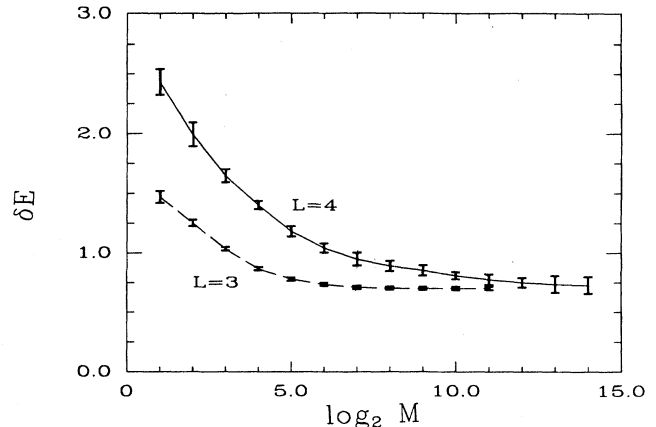


FIG. 1. Effective scaling stiffness energy δE as obtained by Monte Carlo quenches of Gaussian PSG samples. δE is shown vs $\ln_2 M$ where M is the number of Monte Carlo updates per spin. The error bars are based on the finite number of samples considered. The values of L are indicated.

It is harder to establish saturation in systems with the $\pm J$ couplings. Figure 2 shows δE obtained for 200 samples of BPSG with $L=4$. We took $m_0=16$. The saturation is established at $m=15$. In the next section we combine the results of the two methods of deducing the ground-state energy in order to calculate the scaling exponent γ .

V. THE $T=0$ SCALING EXPONENT γ

Consider first the 2D PSG’s. For each $L \times L$ sized system ($L \leq 10$) we took at least 10 000 samples into account. The transfer-matrix results are shown in Fig. 3. Both for GPSG and BPSG a power-law decay is seen. The values of γ are

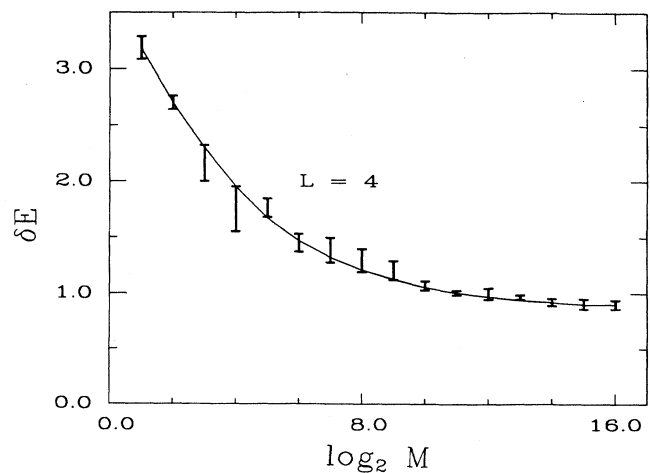


FIG. 2. Similar to Fig. 1 but for bimodal PSG and only for $L=4$.

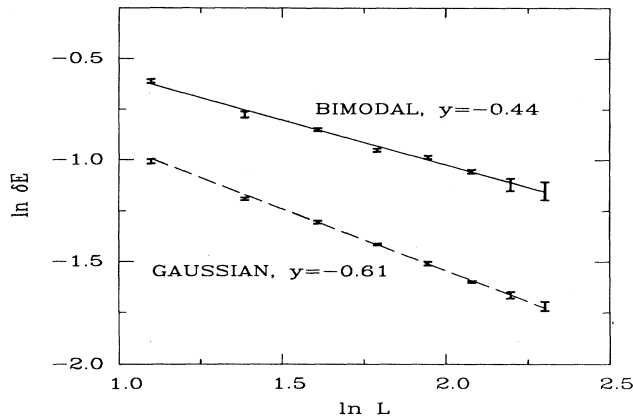


FIG. 3. L dependence of δE for the 2D PSG's. The results are obtained by the transfer-matrix method.

$$y = -0.61 \pm 0.02 \quad (\text{GPSG}, D=2), \quad (6a)$$

$$y = -0.44 \pm 0.03 \quad (\text{BPSG}, D=2). \quad (6b)$$

The error bars have been obtained using the usual statistical measures and are based on the configurational averaging over the distribution of exchange interactions. Systematic errors arising due to small sizes considered are hard to estimate—this remark refers also to all of the data shown from now on.

The first observation stemming from (6) is that 2D PSG's are below the LCD and they will support only a $T=0$ equilibrium phase transition. The second observation is that, very much like the 2D ISG, the bimodal and Gaussian distributions of the couplings give rise to different exponents. This means that for $D=2$ the BPSG and GPSG are in different universality classes. In the ISG case y was found to be ¹² -0.29 for the Gaussian distribution. Thus PSG's have weaker tendencies towards ordering than ISG's.

We shall see in Sec. VI that in the 2D BPSG case the fraction of nonzero effective couplings vanishes with growing L as a power law. This suggests, like in the 2D bimodal Ising case²⁴ that at larger length scales the zero couplings percolate and the system is in fact paramagnetic at $T=0$. Only at shorter length scales it appears spin glassy.

The difference between GPSG and BPSG appears to persist in $D=3$. Figure 4 shows combined results of the transfer-matrix calculations ($L=2,3$; 10 000 samples) and Monte Carlo quenches ($L=4$; 500 samples for GPSG and 200 samples for BPSG) for the 3D Potts spin glasses. We estimate the exponent y to be as follows:

$$y = 0.10 \pm 0.03 \quad (\text{GPSG}, D=3), \quad (7a)$$

$$y = -0.035 \pm 0.06 \quad (\text{BPSG}, D=3). \quad (7b)$$

In the bimodal case the slope of the line joining the $L=3$ and 2 data points is -0.11 ± 0.01 . However, the bimodal system exhibits the "odd-even" effect (see also Fig. 3). To explain this effect consider first blocks of uniform

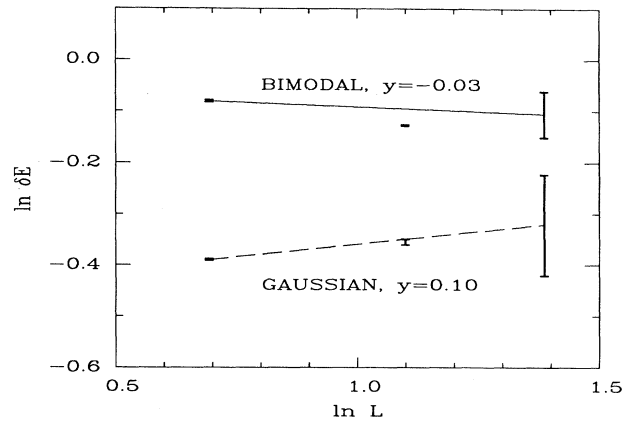


FIG. 4. Dependence of δE for the 3D PSG's. The $L=4$ points have been obtained by Monte Carlo quenches. All other points are results of calculations based on the $T=0$ transfer-matrix approach.

Ising antiferromagnets. Suppose the periodic boundary conditions are imposed in the planes. If L is odd then the planes are always frustrated. This is not the case though if L is even. Thus in order to make calculations of the exponent y , one should separately consider odd and even L . A similar situation is found in bimodal ISG's.¹² In the case of BPSG an extra state "relieves" some of the planar frustration but it is still more reliable to distinguish between odd and even values of L . Unfortunately, the $L=4$ data point is obtained by quenches and that involves much larger error bars than the transfer-matrix method (due to much smaller statistics). Since both the $L=3$ and 4 BPSG have δE lower than that corresponding to $L=2$ we believe that an exactly calculated exponent y is likely to be negative in this case.

In order to obtain an independent measure of y we have performed additional studies of δE for $D=3$. In these studies we keep the transverse area of the system fixed, at $A=3 \times 3$, and we vary only the length l , in the direction along which different boundary conditions are applied. We considered 3100 samples and l was between 3 and 10. In the ordered phase the l dependence is governed by the $\delta E \sim l^x$ law. We obtain $x = -0.97 \pm 0.03$ and -1.04 ± 0.05 for the GPSG and BPSG, respectively, as demonstrated in Fig. 5. One expects, on general grounds,^{10,11,19} that for frustrated systems the A dependence follows the square-root law. The reason is that, on average, half of the interface spins benefit from a change in the boundary conditions and the other half lose. The energy sensitivity to boundary conditions is a fluctuation effect, of order $A^{1/2}$. Altogether this yields

$$\delta E \approx A^{1/2} l^x \quad (8)$$

and

$$y = y_x = (D-1+2x)/2. \quad (9)$$

Thus we get

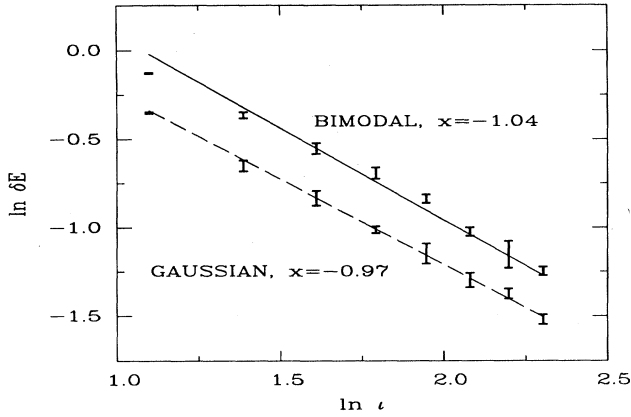


FIG. 5. l dependence of δE for the 3D PSG's for a fixed area of nine spins.

$$y_x = 0.03 \pm 0.03 \quad (\text{GPSG}, D=3), \quad (10a)$$

$$y_x = -0.04 \pm 0.05 \quad (\text{BPSG}, D=3). \quad (10b)$$

We conclude that 3D PSG's are very close to their LCD. At the length scales studied GPSG and BPSG appear to be in different universality classes. The 3D GPSG gives rise to scaling towards a strong coupling at $T=0$, indicating the existence of an equilibrium transition. The 3D BPSG is likely not to have any finite T transition but studying larger length scales might change this point of view.

VI. PROBABILITY DISTRIBUTIONS OF ΔE

The scaling stiffness energy, δE , is a characteristic measure of the sensitivity to changes in the boundary conditions [see Eq. (4)]. It follows that the probability distribution of $|\Delta E|$, in the scaling limit, should be of the form¹²

$$P(|\Delta E|) = \frac{1}{\delta E} f \left(\frac{|\Delta E|}{\delta E} \right). \quad (11)$$

The function $f(x)$ is expected to tend to a fixed shape for $L \rightarrow \infty$.

Figures 6 and 7 seem to indicate that a fixed shape of $f(x)$ is indeed achieved both in the case of $D=2$ and 3 GPSG's. The values of y chosen are those given by (6) and (7), respectively. In both cases $f(x)$ has a Gaussian character. The 3D curve is more concentrated towards the origin than the 2D one but otherwise it is rather similar.

In the case of the bimodal distribution ΔE comes in multiples of J . Following the argument of Bray and Moore,¹² we expect that if y was positive then on a sufficiently large length scale the discretization would become immaterial: the effective coupling becomes larger and larger than J . Thus, for positive y 's, $f(x)$ should be similar to that found for the GPSG. Instead, however, the exponent y is negative in 2D and 3D BPSG. It follows that $P(|\Delta E|)$ narrows increasingly with L . In the

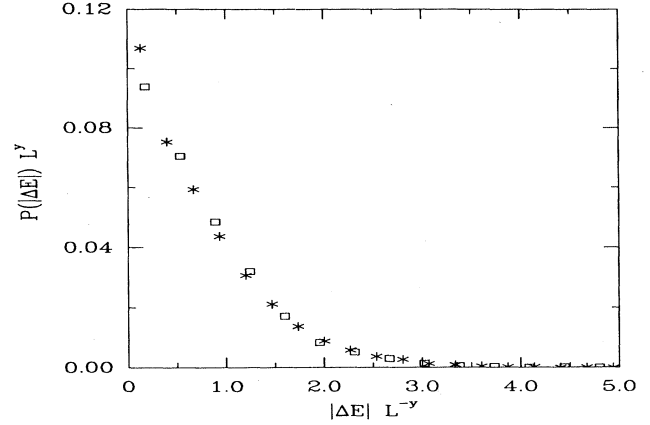


FIG. 6. Scaled distribution function $f(x) = P(|\Delta E|)L^y$ vs $|\Delta E|L^{-y}$ for 2D GPSG. The squares refer to $L=8$ (5000 samples) and asterisks to $L=5$ (10000 samples).

infinite-size limit the fraction of samples with $\Delta E=0$ tends to unity. Thus, the probability $p(L)$ to find a nonzero effective coupling, ΔE , decreases with the size of the system to 0.

A power-law decrease is expected at $T=0$ for systems below the LCD ($y < 0$):

$$p(L) \approx L^{-\eta}. \quad (12)$$

For the 3D BPSG we find $p(2)=0.672$ (statistics of 100 000 samples) and $p(3)=0.668$ (7600 samples). These data are insufficient to determine η but the slight decrease in $p(L)$ would be consistent with a negative value of y .

For the 2D bimodal case we find

$$\eta = 0.42 \pm 0.04 \quad (\text{BPSG}, D=2). \quad (13)$$

This is based on the data points shown in Fig. 8. The statistics here are 10000 samples for $3 \leq L \leq 7$, 3700 for

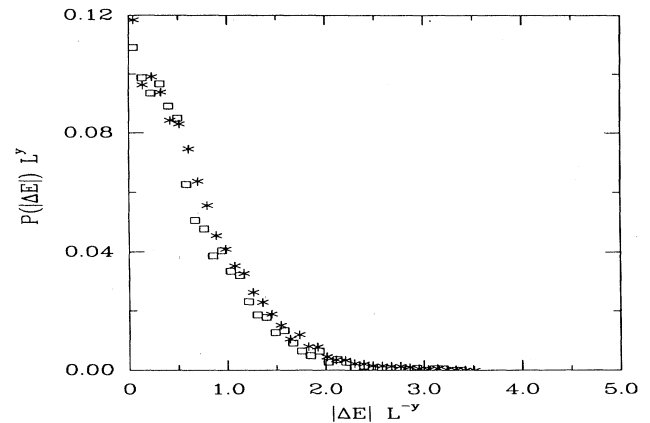


FIG. 7. Similar to Fig. 6 but for 3D GPSG. The squares refer to $L=3$ (5000 samples) and asterisks to $L=2$ (10000 samples).

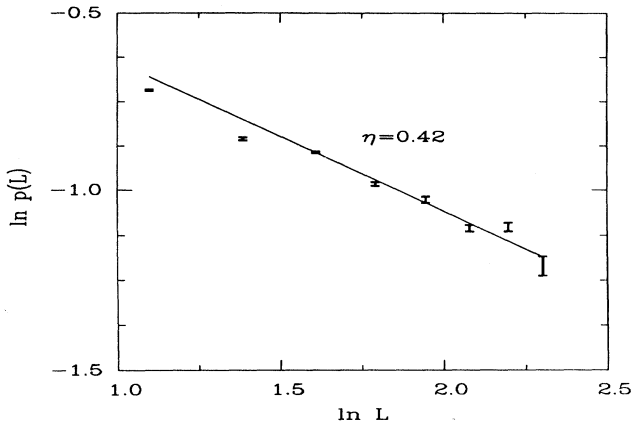


FIG. 8. L dependence of probability to find a nonzero domain-wall energy in 2D BPSG.

$L=8$, 960 for $L=9$, and 440 for $L=10$. It is seen that $p(L)$ displays, weakly, the odd-even effect: samples with an odd number of spins follow a slightly different line than those with an even one. It should be noted that, for the 2D bimodal ISG, $\eta=0.20\pm 0.02$.¹²

The exponent η describes the algebraic decay of the spin-spin correlations. One can see this by the following extension of the argument of Bray and Moore.¹² Since ΔE is an effective coupling, $S_0 S_L$ is nonzero with probability $p(L)$ and 0 with probability $1-p(L)$. A configurational average of $[\langle S_0 S_L \rangle - \langle S_0 \rangle^2]^n$, $n=1, 2, \dots$, yields a constant times $p(L)$. The only distance dependence is contained in $p(L)$. Thus η indeed relates to the spin-spin correlations. The 2D GPSG has a unique ground state and hence $\eta=0$ in this case.

VII. CHAOTIC NATURE OF THE ORDERED PHASE OF GPSG

Ising spin glasses have been found to be chaotic^{19,20} in the sense that the spin order is sensitive to a temperature change δT at length scales L^* of order $(Y/\sigma\delta T)^{1/\zeta}$, where Y and σ are T -dependent amplitudes associated with the interfacial free energy and entropy, respectively. $\zeta=d_S/2-y$ is the Lyapunov exponent characterizing the chaotic behavior and d_S is the fractal dimension of the interface.

The general arguments for chaotic behavior follow from an Imry-Ma¹⁸ argument. We first consider the effect on the ground state of adding a small random perturbation, of relative strength λ , to each bond. Specifically we take

$$J_{ij} \rightarrow J_{ij} + \lambda x_{ij}, \quad (14)$$

with $\lambda \ll 1$ and x_{ij} drawn from a Gaussian pool of couplings with zero mean and unit dispersion. If J is a measure of the width of the unperturbed bond distribution, then the energy cost, in the absence of the perturbation, of a domain of linear extension L is of order JL^y . In the presence of the perturbation, the excitation which originally cost energy may now be energetically favorable,

since there is an additional contribution of order $\pm \lambda JL^{d_S/2}$ from the perturbation where L^{d_S} is the surface area of the excitation. This area is presumably fractal. For 2D ISG $d_S=1.26$ and $d_S/2 > y$. The inequality $\zeta > 0$ is also expected to hold for $D=3$. Thus at sufficiently large L the energy shift is larger than the typical excitation energies in the system and the ground state is unstable against the perturbation on length scales $L > L^* \approx 1/\lambda^{1/\zeta}$. The chaotic response to temperature changes follows immediately from the chaotic response to bond perturbations at $T=0$: Two identical bond distributions at slightly different temperatures T and $T+\Delta T$ are rescaled (in the ordered phase) to two $T=0$ distributions with slightly different bonds. Under subsequent rescaling these pools diverge as discussed above. In this case λ is equal to $\Delta T\sigma/Y$ where σ is the amplitude of the interfacial entropy, $S_{\text{INT}} \approx \sigma(T)L^{d_S/2}$, $L \rightarrow \infty$.

In order to determine d_S one has to calculate the mean interface length and see how it scales with L . An easy way to achieve this, but only in Gaussian systems, is to calculate

$$L_{\text{INT}} = \lim_{\lambda \rightarrow 0} \{ \langle [\Delta E - \Delta E(\lambda)]^2 \rangle_c / \lambda^2 \}, \quad (15)$$

where $\Delta E(\lambda)$ denotes ΔE in the presence of the perturbation (14). This follows from the fact that for a particular sample $\Delta E - \Delta E(\lambda) = (l_{\text{INT}})^{1/2} \lambda z$, where l_{INT} is the actual interface length and z is a normally distributed variable of unit dispersion.

In the case of GPSG one can still calculate a typical effective interface length as defined in Eq. (15) and determine d_S from

$$L_{\text{INT}} \approx L^{d_S} \quad (16)$$

and then deduce the related exponent ζ . However, d_S ceases to have an interpretation of the fractal dimensionality of the interface. Two Potts spins contribute to the energy only if they are in like states. Thus some interface pairs would not respond to the perturbation in

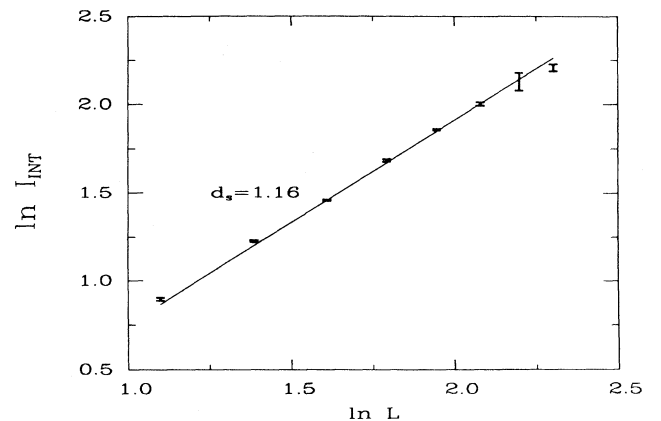


FIG. 9. L dependence of the effective interface length, Eq. (16), for 2D GPSG.

bonds. d_S is therefore an effective fractal dimensionality which enters into the definitions of ζ , the scaling of the interfacial entropy, and the characteristic length scales occurring in response to perturbations. The actual fractal dimensionality of the interface is expected to be larger than or equal to d_S , since the true interface is longer than that estimated using the perturbation (14).

Figure 9 shows the L dependence of the effective interface, Eq. (15), as determined by the transfer-matrix method for the 2D GPSG. The statistics are 10 000 samples for $L \leq 8$, 2800 for $L=9$, and 2000 for $L=10$. The effective fractal dimensionality,

$$d_S = 1.16 \pm 0.06 \quad (\text{GPSG}, D=2) \quad (17)$$

is smaller than for the Ising spins but it is still larger than $2y$. This suggests that GPSG's are also chaotic. We have not obtained d_S for the 3D GPSG but we expect a similar behavior in this case as well.

VIII. CRITICAL TEMPERATURE

The 3D GPSG is slightly above its LCD. The critical temperature of the SG-paramagnet transition is then expected to be small. As T is decreased, the size dependence of the sensitivity to boundary conditions, δF , must cross from a power-law increase to an exponential decay. At T_c δF must be scale invariant.

In order to estimate T_c , we have performed finite T transfer-matrix studies of δF for GPSG on cubes with $L=2$ (10 000 samples) and with $L=3$ (5000 samples). The results are shown in Fig. 10. It is seen that the $L=2$ and 3 lines cross in the vicinity of $T_c=0.27$. This should be considered only as a rough estimate since it is based on studies of δF in very small systems. For ferromagnetic Potts models T_c is of order 1.8.² Thus our value for T_c of GPSG can be considered to be small indeed. Our value of T_c compares well with that of Carmesin and Binder,⁸ who see freezing effects below $T=0.4$.

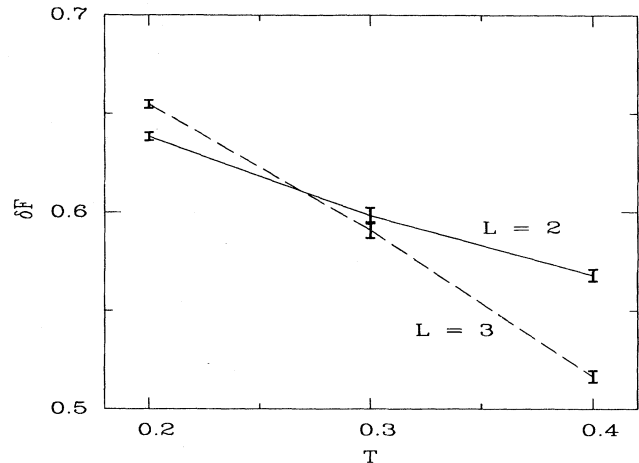


FIG. 10. Temperature dependence of δF for $L=2$ and 3 for 3D GPSG.

IX. CONCLUDING REMARKS

We have seen that, in many ways, short-range Potts spin glasses have properties qualitatively similar to those of short-range Ising spin glasses. The major difference is that the 3D bimodal PSG probably does not have an equilibrium phase transition, unlike the 3D bimodal ISG. It would be interesting to carry out further detailed studies of these systems to elucidate whether they share a common lower critical dimensionality or not. Our calculations suggest that the picture for an Ising spin-glass phase suggested by Fisher and Huse¹⁹ is also valid for PSG's. In particular, PSG's above their LCD would be expected to show an extreme sensitivity of the equilibrium states to small changes in temperature and the SG phase would be destroyed by an arbitrarily weak magnetic field.

ACKNOWLEDGMENTS

One of us (M.C.) was supported by the National Science Foundation, Grant No. DMR-8553271.

*On leave from Institute of Theoretical Physics, Warsaw University, 00-681 Warsaw, Poland.

¹R. B. Potts, Proc. Cambridge Philos. Soc. **48**, 106 (1952).

²F. Y. Wu, Rev. Mod. Phys. **54**, 235 (1982).

³R. J. Baxter, Proc. R. Soc. London, Ser. A **383**, 43 (1982).

⁴J. R. Banavar, G. S. Grest, and D. Jasnow, Phys. Rev. Lett. **45**, 1424 (1980); Phys. Rev. B **25**, 4639 (1982).

⁵R. Kree, L. A. Turski, and A. Zippelius, Phys. Rev. Lett. **58**, 1656 (1987); T. R. Kirkpatrick and D. Thirumalai, Phys. Rev. B **37**, 5342 (1988).

⁶H.-O. Carmesin and K. Binder, Europhys. Lett. **4**, 269 (1987).

⁷D. Elderfield and D. Sherrington, J. Phys. C **16**, L1169 (1983); E. J. S. Lage and J. Nunes da Silva, *ibid.* **17**, L593 (1984); D. J. Gross, I. Kanter, and H. Sompolinsky, Phys. Rev. Lett. **55**, 304 (1985).

⁸H.-O. Carmesin and K. Binder (unpublished).

⁹J. R. Banavar and A. J. Bray, Phys. Rev. B **38**, 2564 (1988).

¹⁰P. W. Anderson and C. M. Pond, Phys. Rev. Lett. **40**, 903 (1978); P. W. Anderson, J. Less-Common Met. **62**, 291 (1978).

¹¹J. R. Banavar and M. Cieplak, Phys. Rev. Lett. **48**, 832 (1982); J. Phys. C **16**, L755 (1983).

¹²A. J. Bray and M. A. Moore, in *Heidelberg Colloquium on Glassy Dynamics*, edited by L. Van Hemmen and I. Morgenstern (Springer, Berlin, 1987), p. 121; J. Phys. C **17**, L463 (1984).

¹³W. L. McMillan, Phys. Rev. B **30**, 476 (1984).

¹⁴B. W. Morris, S. G. Colborne, M. A. Moore, A. J. Bray, and J. Canisius, J. Phys. C **19**, 1157 (1986).

¹⁵K. Binder and A. P. Young, Rev. Mod. Phys. **58**, 801 (1986).

¹⁶R. N. Bhatt and A. P. Young, Phys. Rev. Lett. **54**, 924 (1985); A. Ogielski and I. Morgenstern, *ibid.* **54**, 928 (1985).

¹⁷R. E. Walstedt and L. R. Walker, Phys. Rev. Lett. **47**, 1624

- (1981); K. Binder, *Z. Phys.* **48**, 319 (1982); M. Z. Cieplak and M. Cieplak, *J. Phys. C* **17**, 2933 (1984); J. A. Olive, A. P. Young, and D. Sherrington, *Phys. Rev. B* **34**, 6344 (1986); A. Chakrabarti and C. Dasgupta, *Phys. Rev. Lett.* **56**, 1404 (1986).
- ¹⁸Y. Imry and S.-K. Ma, *Phys. Rev. Lett.* **35**, 1399 (1975).
- ¹⁹D. S. Fisher and D. A. Huse, *Phys. Rev. Lett.* **56**, 1601 (1986); D. A. Huse and D. S. Fisher, *Phys. Rev. B* **35**, 6841 (1987); D. S. Fisher and D. A. Huse, *ibid.* **38**, 386 (1988).
- ²⁰A. J. Bray and M. A. Moore, *Phys. Rev. Lett.* **58**, 57 (1987); J. R. Banavar and A. J. Bray, *Phys. Rev. B* **35**, 8888 (1987); A. J. Bray, *Comments Cond. Mat. Phys.* **14**, 21 (1988); note also that chaotic behavior was first observed in a hierarchical Ising model with competing interactions by S. McKay, A. N. Berker, and S. Kirkpatrick, *Phys. Rev. Lett.* **48**, 767 (1982). The origins of the chaos seem different in the two cases.
- ²¹R. G. Caflisch, J. R. Banavar, and M. Cieplak, *J. Phys. C* **18**, L991 (1985).
- ²²J. R. Banavar and M. Cieplak, *Phys. Rev. B* **39**, 9633 (1989).
- ²³I. Morgenstern and K. Binder, *Phys. Rev. B* **22**, 288 (1980).
- ²⁴M. Cieplak and J. R. Banavar (unpublished).